

# ULTIMATE STRENGTH AND POSTBUCKLING STIFFNESS OF PLATE PANELS SUBJECTED TO COMBINED LOADS USING SEMI-ANALYTICAL MODELS

Eivind Steen\* and Eirik Byklum\*

\*Section for Hydrodynamics, Structures and Stability, Det Norske Veritas, Norway

## SUMMARY

Non-linear semi-analytical buckling models are developed for fast and accurate buckling, postbuckling and ultimate strength assessment of thin-walled plate panels. The models are founded on thin-walled large deflection plate theory, Raleigh-Ritz discretization of the buckling deflection and incremental methods for solving the geometrically non-linear equilibrium equations. By limiting the degrees of freedom and solving the non-linear geometrical problem, combined with hot spot stress control of the redistributed stress pattern, buckling and ultimate strength limits are estimated with good accuracy and a minimum of computer effort. The models are packed into simple user interface tools (PULS) for easy physical interpretation of buckling characteristics. Examples are presented illustrating typical features of non-linear behaviour of plates subjected to combined bi-axial and shear loads and some comparisons with full blown non-linear finite element codes are included. Comparisons with existing Classification rules are also included for some cases.

## 1. INTRODUCTION

Design of stiffened panels and girders in ship structures to sustain compressive forces is the main criterion defining the necessary dimensions of the plating as well as the stiffening elements. Likewise after several years in service, corrosion wear and tear is unavoidable and makes the structure thinner and more vulnerable to buckling and collapse. These concerns support the consensus among researchers, designers and rule makers that buckling and ultimate strength limit states are the most important criteria in any safety and risk assessment of ships operating in a seaway.

Moreover, critical load bearing elements in ship hulls, such as in bottom, deck and ship side, will be exposed to a complex stress pattern with simultaneously acting stresses in bi-axial directions as well as in-plane shear stresses and lateral pressure. To determine buckling and ultimate strength of elements subjected to such combined local stress effects is very complicated. The standard approach is to use approximate empirical formulas provided by Classification Societies and neglect load history effects linked to phase differences between dynamic stresses acting in the different plate directions. Such methods are known to be rather inaccurate though mostly on the conservative side.

Resort to advanced non-linear FE analysis tools are only seldom done, partly due the uncertain load history as well as due to the software expert level, time and costs required.

However, with the recent development of computers, it has become feasible to make more direct use of non-linear buckling theory programmed and packed into simple to

understand software. This is the main idea behind the new buckling code package PULS developed by Det Norske Veritas Ref. (10). By using advanced semi-analytical models the designers and engineers will not only be able to quickly and more accurately assess the strength of the structure, but they will also gain an improved understanding of the physics involved since 3D graphical features illustrating failure modes and stress redistributions are readily available. Deeper insight and understanding among non-experts will give more robust design solutions with more optimal and effective use of the material.

This paper gives a brief description of the different elements implemented in PULS, with some examples showing the characteristics of buckling, postbuckling and non-linear behaviour.

More details related to the different PULS buckling models and theory can be found in Refs. (3),(4),(5),(6),(7),(8),(13),(14),(15),(16) More info and publications can be found on [www.dnv.com](http://www.dnv.com).

## 2. DESCRIPTION

There are currently three different buckling models developed for the PULS code. The unstiffened plate model is illustrated in Fig.1 (U3 element), the regularly stiffened plate model is illustrated in Fig.2 (S3 element), and the non-regular geometry model is illustrated in Fig. 3 (T1-element).

The unstiffened plate model (U3) is applicable for plates where the edges are known to have rigid support in the

lateral direction. It should therefore normally not be used for plate fields between stiffeners unless the stiffeners are sufficiently strong. The element assesses elastic buckling as well as post-critical strength and is thus suited for ultimate limit state design.

The regularly stiffened plate model (S3) also assume the outer plate edges to have rigid support in the lateral direction and is thus suited for internal integrated plate fields between strong frame structures such as in ship deck, bottom, tank top, ship sides etc. The stiffening system may be uni-directional or orthogonal, with the continuous plating and primary stiffeners as the main load bearing elements. Secondary stiffeners running perpendicular to the primary direction act as buckling stiffeners and do not carry loads themselves. The element assesses elastic buckling as well as post-critical strength and is thus suited for ultimate limit state design.

The plate model developed for non-regular geometry (T1) is based on a linearized plate theory. Hence, it is useful for areas of a ship hull with complex geometry, and for design of structural components in which no elastic buckling and large deflections are accepted. This may typically be girder webs, stringer decks, aft and fore ship parts etc.

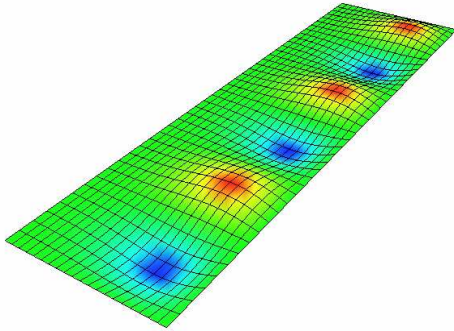


**Fig. 1 PULS unstiffened plate model (U3)**

All three models cover load combinations such as bi-axial compression/tension, in-plane shear and lateral pressure loads as typical for panels in ship deck, bottoms, sides etc. Linearly varying stress along an edge may also be considered for some cases.

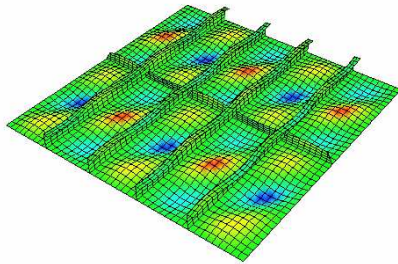


**Fig. 2 PULS regularly stiffened plate model (S3)**

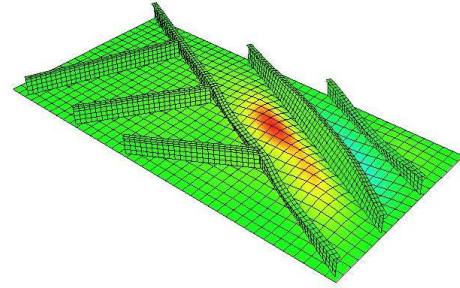


**Fig. 3 PULS non-regular geometry model (T1)**

### 3. THEORY

#### 3.1 GENERAL

The PULS buckling models can be classified as semi-analytical in the sense that they are based on recognized non-linear plate theory using trigonometric functions and multiple degrees of freedom series for describing the buckling deflections. For problems which can be analysed with sufficient accuracy using few or only a single degree of freedom the buckling and post-buckling behaviour resemble classical analytical solutions found in the literature and standard textbooks such as Refs. (2),(17).

The set of non-linear equilibrium equations is solved using an incremental numerical perturbation scheme with arc length control and the equilibrium path in solution space is traced along the specified load history. Using the non-linear plate theory, second order membrane strains and redistribution of membrane stresses are accounted for. The equivalent von Mises yield stress in hot spot locations is controlled against the material yield condition. The elastic buckling limit, post-critical response and ultimate strength is assessed.

#### 3.2 BASIC THEORY

The theory is given detailed treatment elsewhere, so only some of the basics are given here. The fundamental non-linear plate theory is due Marguerre, Ref.(11), with well known kinematic and compatibility equations

$$\begin{aligned}\epsilon_{11} &= u_{,1} + \frac{1}{2} w_{,1}^2 + w_{,1} w_{0,1} \\ \epsilon_{22} &= u_{,2} + \frac{1}{2} w_{,2}^2 + w_{,2} w_{0,2} \\ \epsilon_{12} &= \frac{1}{2} (u_{,1,2} + u_{,2,1}) + \frac{1}{2} (w_{,1} w_{,2} + w_{,1} w_{0,2} + w_{,2} w_{0,1})\end{aligned}\quad (1)$$

$$\nabla^4 F = E [w_{,12}^2 - w_{,11} w_{,22} + 2w_{0,12} w_{,12} - w_{0,11} w_{,22} - w_{0,22} w_{,11}] \quad (2)$$

The  $\varepsilon_{\alpha\beta}$  are the membrane strain tensor,  $u_{\alpha,\beta}$  the in-plane displacement gradients and  $w_{,\alpha}$ ,  $w_{,\alpha\beta}$ ,  $w_{0,\alpha}$ ,  $w_{0,\alpha\beta}$  the additional and initial out-of plane plate deflection gradients ( $\alpha, \beta = 1, 2$ ), and  $F$  is the Airy's stress function.

The lateral buckling deflections  $w$  due to applied loads and initial stress free geometrical imperfections  $w_0$  are represented by double Fourier series ( $i, j = 1, 2, \dots, N$ ).

$$w = q_i f_i(x_1, x_2) = \sum_m \sum_n A_{mn} \sin\left(\frac{m\pi}{a} x_1\right) \sin\left(\frac{n\pi}{b} x_2\right) \quad (3)$$

$$w_0 = q_{i0} f_i(x_1, x_2) = \sum_m \sum_n A_{mn}^0 \sin\left(\frac{m\pi}{a} x_1\right) \sin\left(\frac{n\pi}{b} x_2\right)$$

The equilibrium equations are derived on an incremental form using energy principles. This means that the rates of deflection of the parameters  $A_{mn}$  with respect to the arc length variable  $\eta$  along the equilibrium path in solution space, i.e. the  $\dot{A}_{mn}$  coefficients, are the unknowns. The perturbation expansion provides a linearized set of  $N$  equations in  $N+1$  unknowns ( $N$  is the total set of  $A_{mn}$  coefficients,  $A_{11}, A_{12}, \dots$ , etc.). The final equation comes from the definition of the arc length parameter  $\eta$  and gives a single quadratic equation in the unknown rate coefficients. The final set of equations are compactly written as

$$K_{ij} \dot{q}_j + G_{i\Lambda} \dot{\Lambda} = 0 \quad i, j = 1, 2, \dots, N \quad (4a)$$

$$\dot{q}_i \dot{q}_i + \dot{\Lambda}^2 = 1 \quad (4b)$$

Here  $K_{ij}, G_{i\Lambda}$  are the state dependent geometrical stiffness matrix and incremental load vector, respectively. The  $\dot{q}_i$ 's are the unknown deflection rate parameters and  $\dot{\Lambda}$  the load rate respectively in the series expansion

$$\begin{aligned} q_{1,s+1} &= A_{11,s+1} = A_{11,s} + \dot{A}_{11,s} \Delta\eta + \dots \\ q_{2,s+1} &= A_{12,s+1} = A_{12,s} + \dot{A}_{12,s} \Delta\eta + \dots \\ &\vdots \\ \Lambda_{s+1} &= \Lambda_s + \dot{\Lambda}_s \Delta\eta + \dots \end{aligned} \quad (5)$$

The sub index  $s$  on the variables indicates state  $s$ , index  $s+1$  the next neighbouring state  $s+1$  and  $\Delta\eta$  is the incremental prescribed arc length parameter along the equilibrium path.

The unit load parameter  $\Lambda$  is defined as the load factor scaling all  $K$  external loads  $\sigma_1, \sigma_2, \dots, \sigma_K$  in the same proportion, i.e.

$$\begin{aligned} \sigma_1 &= \Lambda \sigma_{10} & \dot{\sigma}_1 &= \dot{\Lambda} \sigma_{10} \\ \sigma_2 &= \Lambda \sigma_{20} & \dot{\sigma}_2 &= \dot{\Lambda} \sigma_{20} \\ &\vdots & &\vdots \\ \sigma_K &= \Lambda \sigma_{K0} & \dot{\sigma}_K &= \dot{\Lambda} \sigma_{K0} \end{aligned} \quad (6)$$

The  $\sigma_1$  is typically the axial load,  $\sigma_2$  the transverse load acting perpendicular to  $\sigma_1$ ,  $\sigma_3$  is the shear stress etc.

The non-linear equilibrium path is traced solving the equilibrium equations in an incremental scheme. The parameter rates in state  $s$  are directly used for finding deflections and the loads for the next state  $s+1$ . Moreover, only the first order rates in the perturbation expansion are used together with a very small value of the incremental perturbation parameter  $\Delta\eta$ . It is generally found that  $\Delta\eta \approx 0.01$  gives sufficiently accurate solutions.

By checking the redistributed stress pattern against the von Mises yield criterion in critical locations inside the panel and along plate edges the localized material plastification is under control at each load step. When the first onset of material yield is reached the incremental loading is stopped and the corresponding total load is defined as the ultimate capacity. This approach thus neglects the spread of plasticity both across the plate thickness and in-plane direction and this saves a significant amount of computer time. Moreover, used in an ultimate limit state context the present approach prevents major permanent sets and buckles.

### 3.3 MODEL RESULTS

The non-linear solution algorithm identifies the value of load parameter  $\Lambda$  to be  $\Lambda_u$  at the ultimate capacity limit. The corresponding ultimate strength values of the external loads are accordingly

$$\begin{aligned} \sigma_{1u} &= \Lambda_u \sigma_{10} \\ \sigma_{2u} &= \Lambda_u \sigma_{20} \\ &\vdots \\ \sigma_{Ku} &= \Lambda_u \sigma_{K0} \end{aligned} \quad (7)$$

The ultimate capacity factor  $\Lambda_u$  is directly a measure of the safety margin against collapse. The inverse of this factor is the actual usage factor commonly used in Ship Classification rules, i.e.

$$\eta = \frac{1}{\Lambda_u} = \frac{\sqrt{\sigma_{10}^2 + \sigma_{20}^2 + \dots + \sigma_{K0}^2}}{\sqrt{\sigma_{1U}^2 + \sigma_{2U}^2 + \dots + \sigma_{KU}^2}} \quad (8)$$

The concept of usage factor is illustrated schematically in load space ( $\sigma_1, \sigma_2, \sigma_3$ ) in Fig. 4. A similar definition for usage factor against the elastic buckling limit is straightforward substituting the eigenvalue factor  $\Lambda_E$  for  $\Lambda_u$ .

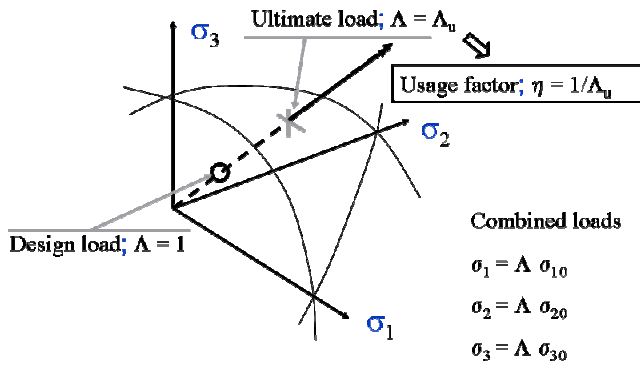


**Fig. 4. Ultimate Capacity failure surface in load space. Proportional load history and definition of usage factor  $\eta$ .**

## 4. EXAMPLES

### 4.1 UNSTIFFENED PLATE (U3)

Square plate:

A square plate is analysed under balanced 50 - 50 % bi-axial compression. The plate dimensions are 1000x1000x17 mm, material Young's modulus  $E=210000$  MPa., Poisson's ratio  $\nu = 0.3$ , yield stress = 315 MPa.

The purpose of the analyses was to investigate the loss of in-plane stiffness after the elastic buckling limit is passed. Since the loss of stiffness is most marked for geometrically perfect plates an imperfection amplitude of 1% of the plate thickness was specified in the mode  $m = 1, n = 1$  ( $A_{11}^0 = 0.17\text{mm}$ , rest  $A_{mn}^0 = 0$ ).

The load-shortening curves are shown in Fig.5 illustrating the significant drop in membrane stiffness beyond the elastic buckling stress of 110 MPa. The uni-axial compression case is known to have a stiffness drop of 50% beyond the eigenvalue, see e.g. Rhodes (1982) while the present bi-axial compression case shows a 75% stiffness drop. Fig. 5 also shows the close resemblance between the present semi-analytical solution (Byklum 2002C, a closed form solution Steen(1998) and the ABAQUS results. Included in the figure is also the ultimate capacity predicted by PULS which compares favourably with ABAQUS ultimate capacity. The ABAQUS model applies a mesh using 8x8 elements of the S4R type.

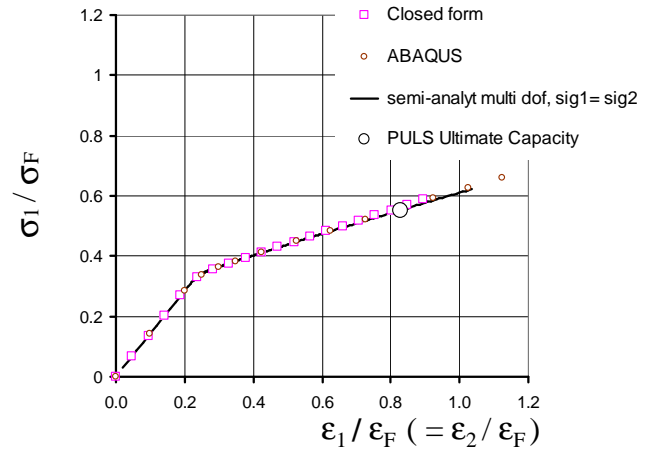


**Fig. 5. Load-shortening curves and comparison between present analytical multi-dof solution, closed form solution and ABAQUS.**

The redistributed membrane stress distribution at ultimate capacity is illustrated in Fig. 6, i.e. the von Mises stress in a) and the normal membrane stress in b). The accumulation of stresses along the edges and high equivalent von Mises particularly in the corner are clearly illustrated

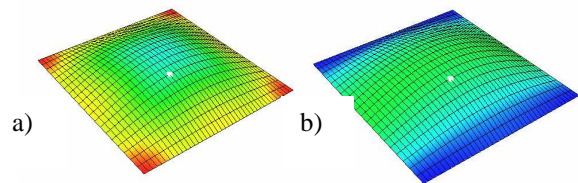


**Fig. 6. Redistributed membrane stress at ultimate capacity, a) von Mises, b) normal stress**

The square plate is also analyzed under a set of proportional loading histories as to find the ultimate capacity for all bi-axial load combinations, compression-compression as well as compression-tension and tension-tension. Fig. 7 shows the ultimate capacity and eigenvalue curve predicted by the present model. This way of presenting strength in load space is illustrative and by adding the eigenvalue curve it is shown that even plates with moderately thickness of 17 mm has a relatively large area in which the plates may operate in the postbuckling region without suffering permanent sets (overcritical strength). The straight line emanating from origin represents the balanced 50-50 bi-axially compression case.

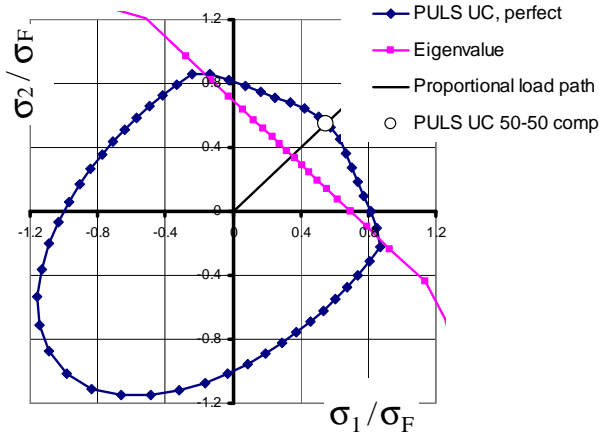


**Fig. 7. Ultimate Capacity and eigenvalue limits in the bi-axial ( $\sigma_1 - \sigma_2$ ) load space predicted by PULS.**

Fig. 8 show bi-axial ultimate capacity curves for the same plate, but with simultaneously acting fixed shear stress levels of 50, 100 and 150 MPa. It is demonstrated that the presence of shear stresses eat off the bi-axial capacity, but more so in the tension region than in the compression region.

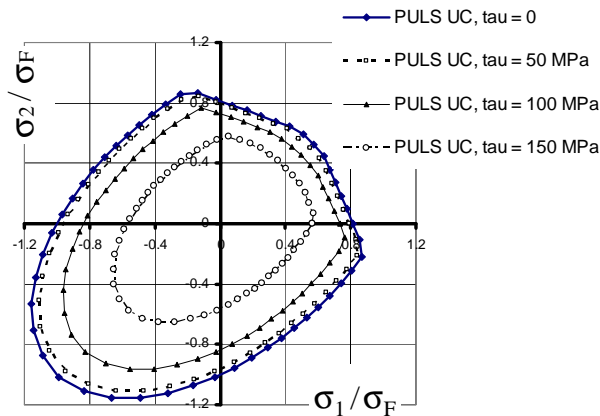


**Fig. 8. Ultimate Capacity limits in the bi-axial ( $\sigma_1 - \sigma_2$ ) load space with fixed shear stresses, 50, 100, 150 MPa as predicted by PULS.**

Rectangular plate:

A rectangular plate is analysed under a set of different proportional load histories for scanning the bi-axial compression-compression strength. The plate dimensions are 2400x800x20 mm, material Young's modulus  $E=208000$  MPa, Poisson's ratio  $\nu = 0.3$ , yield stress = 235 MPa. Default PULS model tolerance was used, i.e. an amplitude of  $b/200 = 4$  mm in the most critical modes.

The purpose of the analyses was to investigate the ultimate capacity and to compare the results with ABAQUS and existing DNV ship rules. The results are presented in Fig. 9.

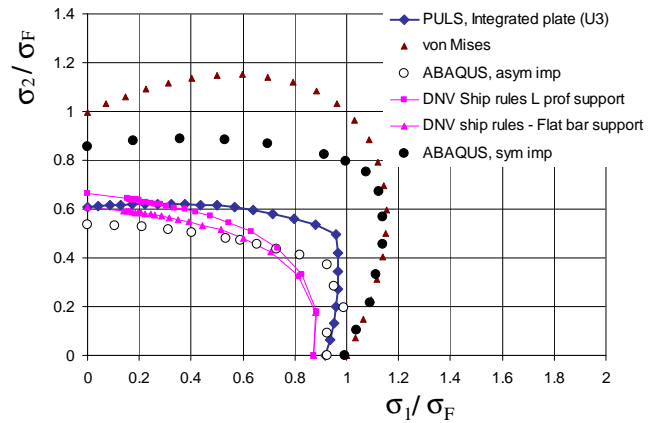


**Fig. 9. Ultimate Capacity limits in the bi-axial ( $\sigma_1 - \sigma_2$ ) load space for an unstiffened plate. Comparisons between PULS, ABAQUS and DNV Rules, Ref.(9).**

Two ABAQUS models are run, one with asymmetric imperfections across the longitudinal edges. As seen the difference in strength is significant. The former imperfection form represent the lower bound strength limit and the latter the upper bound strength limit. The PULS ultimate strength for integrated plates lay in-between, closer to the ABAQUS lower bound results.

The membrane stress distribution at ultimate capacity is illustrated in Fig. 10 for pure axial compression in a) and for pure transverse compression in b).

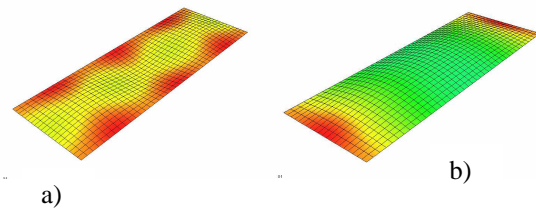


**Fig. 10 Redistributed von Mises membrane stress at ultimate capacity, a) pure axial compression, b) pure transverse compression**

#### 4.2 REGULARLY STIFFENED PLATE (S3)

The regularly stiffened panel is the most important structural element in a ship hull and its buckling and ultimate strength limit is of vital importance. The PULS S3 element offers an accurate and reliable assessment of the strength with due consideration of all relevant buckling modes such as local plate buckling between stiffeners, local buckling of stiffener web plate, torsional/sideways buckling of stiffeners and global/overall buckling of the whole stiffened panel. All these modes may interact and stress redistributions between plating and stiffeners may take place for high

compressive loads. Such interactive effects are generally not considered in standard rule formulations offered by Classification Societies.

The direct application of non-linear plate theory, however, makes it feasible to include all non-linear interactive effects in a theoretically consistent way.

As an example stiffeners are attached to the rectangular unstiffened plate analyzed in the first part herein. Two different panels with different stiffener sizes are analyzed under a set of proportional bi-axial compression loads. Large stiffener: L-profile with 350x120x15x20 mm. Small stiffener: L-profile with 150x50x15x20 mm. Both set of stiffeners have a yield stress of  $\sigma_F = 235$  MPa, and five stiffeners are used equally spaced across the plating.

The results are shown in Fig.11 in the full bi-axial compression quadrant. The superior strength of large stiffeners is clearly demonstrated for all load combinations. Included for reference is also the strength of the simply supported unstiffened plate between stiffeners copied directly from Fig.9. It is seen that the axial capacity of the plate between the stiffeners is very close to the total axial capacity of the stiffened panel indicating that there is marginal redistribution of stresses between plate and stiffeners. This is as expected for this example since the lowest eigenvalue is well above the yield stress.

Obviously, the main reason for the less strength of the stiffened panel with small stiffeners is the tendency of the stiffeners to buckle out-of-plate in a global mode together with plating. The global stiffener deflections, though moderate in size for normal ship design panels as these, do induce bending stresses across the stiffener height which again triggers the early collapse. Fig.12. shows the collapse modes for the axially compressed panels, and it is seen that for both panels the local plate deflections between the stiffeners dominate over the lateral stiffener deflections. Some more flexing deflections of the small stiffener case may be seen.

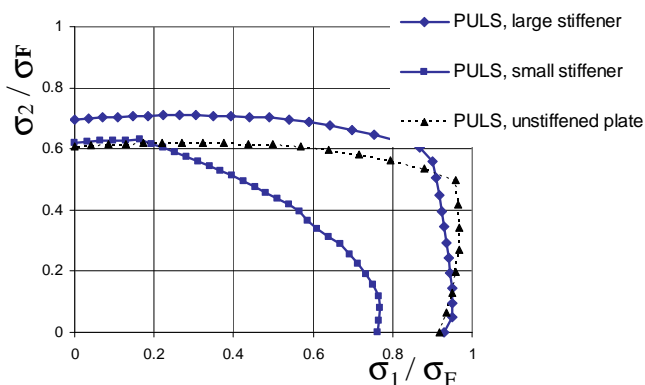


**Fig. 11. Ultimate Capacity limits in the bi-axial ( $\sigma_1 - \sigma_2$ ) load space of stiffened panels with large and small stiffeners.**

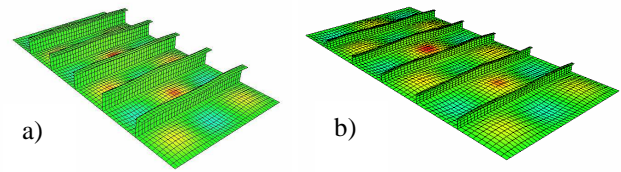


**Fig. 12. Ultimate Collapse mode of axially compressed panels. a) large stiffeners, b) small stiffeners**

#### 4.3 NON- REGULARLY STIFFENED PLATE (T1)

A special element for non-regular stiffening arrangements of plates has been developed. Non-regular stiffening is typical for girder structures, stringer decks, fore and aft peak structures etc. The present element can handle complex geometry such as inclined stiffener orientations encapsulating triangular, trapezoidal plate shapes etc. Different stiffener proportions on the same plate are also coped with.

If such structural elements are not accepted to buckle elastically, even if extreme environmental loads are considered, a simplified theoretical treatment is feasible. The approach used here is a linearization of the equilibrium equations combined with Marguerre's compatibility equation for assessing the redistributed membrane stress distribution. In combination these assumptions allow for a consistent calculation of hot spot von Mises stresses and elastic buckling and material yield plateau emerges as design limits. The linearized theory implies that loads beyond the minimum eigenvalue can not be carried and the plate is assumed to be the active load carrying part while the stiffeners act as buckling stiffeners carrying no loads themselves.

As an example a typical transverse girder web between outer bottom and tank top is analysed. The plating has dimension 5000x1500x15mm with four sniped flatbar profiles 150x15 with spacing 1000 mm, spanning the girder height of 1500 mm. The longitudinal stiffeners running along the tank top is fictively modelled as four short infinitely stiff elements of height 300 mm clamping the plate locally at these positions. The similar long stiffeners running along the bottom plate is not considered here.

The structural configuration and the corresponding buckling modes for pure axial compression and pure shear loading are shown in Fig. 13 and Fig. 14 respectively.

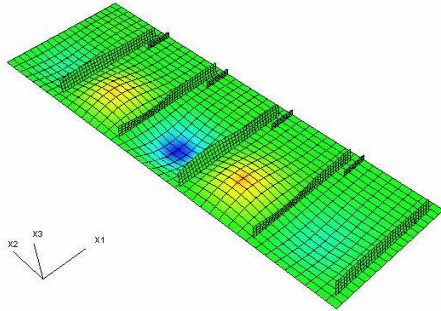


**Fig. 13. Buckling mode for axial compression load  $\sigma_1$**

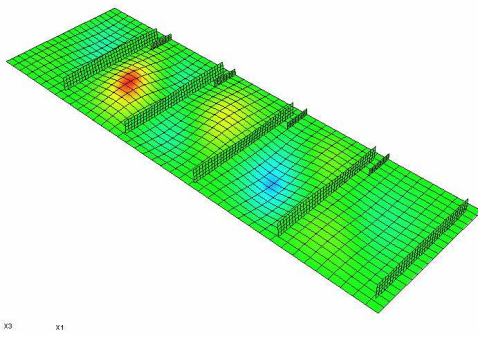


**Fig. 14. Buckling mode for shear loading  $\tau$**

These figures show the influence of the localized clamping along one edge to be significant for the axial compression case while less so for the shear loading.

Transverse girder web plates are normally subjected to a combined stress situation with dominant axial loading and shear with possibly some additional transverse compression. To investigate the buckling strength under such combined load situations the panel is analysed for a set of proportional load histories covering the full range of stress combinations in load space ( $\sigma_1 - \tau$ ) with zero and fixed transverse stress  $\sigma_2 = 50$  MPa acting simultaneously. The results are shown in Fig. 15. It is demonstrated that for axial and transverse dominating loads the buckling effect is significant and strength close to eigenvalue, while for shear dominant loading the buckling strength is higher and the failure is more dominated by material yielding.

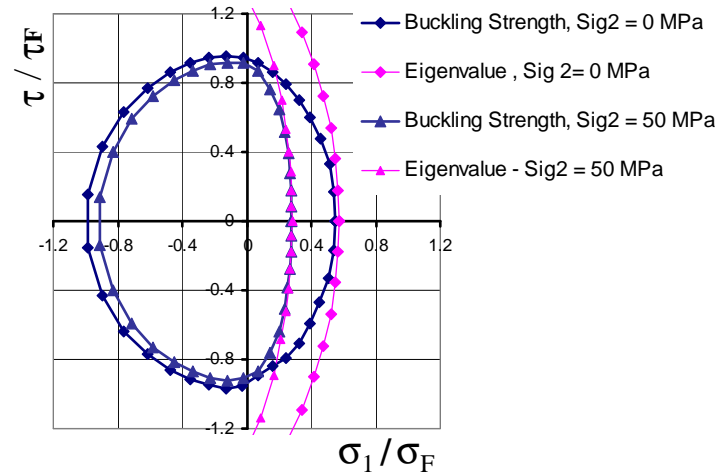


**Fig. 15. Buckling and eigenvalue capacity curves in axial-shear ( $\sigma_1 - \tau$ ) load space with zero and fixed transverse stress  $\sigma_2 = 50$  MPa**

Fig 15 also shows that the axial buckling capacity is significantly reduced by the presence of a transverse compressive stress of  $\sigma_2 = 50$  MPa. Fig. 16 below shows the buckling mode for the case of axial/transverse stress ratio of 2:1 (100/50 MPa at buckling). It is observed that the localized clamping along one plate edge is not disturbing the natural long waved buckling shape as typically seen for axial dominating loading, ref. Fig.13. This is the reason for the relatively large knock down effect on the axial buckling capacity when transverse stresses act simultaneously.

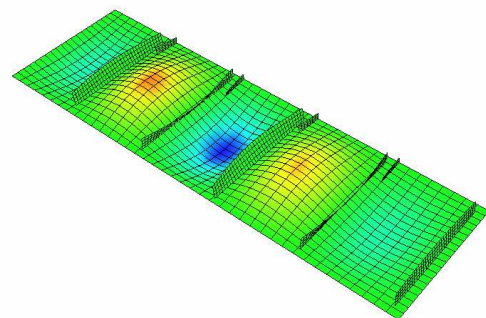


**Fig. 16. Buckling mode for combined axial and transverse compression loads in proportion 2:1**

## 5. CONCLUSIONS

Direct calculation models for buckling and ultimate capacity assessment of stiffened panels are presented. The basic theory is founded on energy principles and nonlinear plate theory and the main approach is given a brief description. Three different plate models are developed and implemented into the computer code PULS offered by Det Norske Veritas.

The direct calculation approach gives increased accuracy compared with conventional empirical based rule formulas. This is especially true for combined load situations and for non-regular geometries for which the

explicit rule design formulas are not intended for. Using advanced buckling theory more information is also available in form of displacement shapes and size, redistributed stress patterns etc. all features which improves and highlight the physical behaviour.

The presented examples focus and demonstrate several relevant aspects of buckling and non-linear behaviour such as the elastic buckling limit, postbuckling stiffness and combined load effects.

Validation of the method is performed by use of nonlinear finite element calculations (ABAQUS (2005)). Comparisons are also made with existing ship rules used by Classification Societies for some examples.

## Acknowledgement

A special thank goes to our colleagues Kjetil G. Vilming, DNV and Lars Brubak, University of Oslo (UiO) for their theoretical development and programming efforts. Thanks also to B.C. Simonsen, S. Valsgård, G. Holtsmark and Å. Bøe all in DNV for their continuous technical support. Discussions with professor J. Helleland at UiO and professor J. Amdahl at NTNU (Trondheim) are also highly appreciated. Thanks also to Rune Torhaug and Eirik Andreassen at DNV for their continuous backing of the present developments.

## References

1. ABAQUS (2005), Version 6.5, *User's Manual*, Hibbitt, Karlsson & Sorensen, Inc. 2005, USA
2. Brush, D.O. and Almroth, B.O. (1975) "Buckling of Bars, Plates, and Shells". McGraw-Hill, International student edition.
3. Brubak, L. Helleland, J., Steen, E. and Byklum, E. (2004). "Approximate buckling strength analysis of plates with arbitrarily oriented stiffeners". Proceedings of the 17<sup>th</sup> Nordic Seminar on Computational Mechanics (NSCM-17), KTH mechanics, Stockholm, 15-16 Oct. 2004.
4. Brubak, L. Helleland, J. (2005). "Computational buckling strength analysis of stiffened plates with varying thickness". International Conference on Computational methods in Marine Engineering. MARINE2005, Eccomas thematic Conference Oslo, Norway 27-29 June.
5. Byklum, E, and Amdahl, J (2002A). "Nonlinear buckling analysis and ultimate strength prediction of stiffened steel and aluminium panels". The Second Int. Conference on Advances in Structural Engineering and Mechanics, Busan, South Korea, 2002.
6. Byklum, E, and Amdahl, J (2002B) "A simplified method for elastic large deflection analysis of plates and stiffened panels due to local buckling". Thin Walled structures, Vol. 40 (11), pp 923-951.
7. Byklum, E (2002C). "Ultimate strength analysis of stiffened steel and aluminium panels using semi-analytical methods". Phd thesis, Norwegian University of Science and Technology, Trondheim, Norway.
8. Byklum, E, Steen, E, and Amdahl, J (2004) "A semi-analytical model for global buckling and postbuckling analysis of stiffened panels". Thin Walled structures, Vol. 42 (5), pp 701-717.
9. Det Norske Veritas (2004). Rules for Classification of Ships.
10. Det Norske Veritas (2004) Report no. 2004-0406. "PULS 2.0 – User's manual"
11. Marguerre, K. (1938). "Zur theorie der gekrümmten platte grosser formeändrug", Proceedings of the 5<sup>th</sup> international congress for applied mechanics, p. 93-101.
12. Rhodes, J. (1982). "Effective widths in plate buckling". Chap 4 in Developments in Thin-Walled Structures-1, Editors: Rhodes, J. and Walker, A.C. ,Applied Science Publishers, London.
13. Steen, E. (1998). Application of the Perturbation Method to Plate Buckling Problems. Research Report in Mechanics, No. 98-1. Mechanics Division, Department of Mathematics, University of Oslo, ISSN 0801-9940, ISBN 82-553-1149-1.
14. Steen, E, Østvold, TK and Valsgård, S (2001). "A new design model for ultimate and buckling strength assessment of stiffened plates". PRADS 2001, Shanghai.
15. Steen, E, Byklum, E and Vilming KG(2004) , "Computer Efficient Non-Linear Buckling Models for Capacity Assessments of Stiffened Panels Subjected to Combined Loads", ICTWS 2004 Conference, Loughborough, UK.
16. Steen, E, Byklum, E., Vilming, K.G., Østvold, T.K. "Computerized buckling model for ultimate strength assessment of stiffened ship hull panels", PRADS 2004 conference, Travemunde/Lubeck.
17. Timoshenko, S. P. and Gere, J.M. (1961) "Theory of Elastic Stability ". McGraw-Hill, International Student Edition.